Hyaluronan Derived From the Limbus is a Key Regulator of Corneal Lymphangiogenesis

Mingxia Sun,[1] Sudan Puri,[1] Kazadi N. Mutoji,[1] Yvette M. Coulson-Thomas,[2] Vincent C. Hascall,[3] David G. Jackson,[4] Tarsis F. Gesteira,[1,2] and Vivien J. Coulson-Thomas[1]

[1]College of Optometry, University of Houston, Houston, Texas, United States
[2]Universidade Federal de São Paulo, São Paulo, Brazil
[3]Cleveland Clinic, Cleveland, Ohio, United States
[4]MRC Human Immunology Unit, University of Oxford, Oxford, United Kingdom

Correspondence: Vivien J. Coulson-Thomas, University of Houston, College of Optometry, 4901 Calhoun Road, Houston, TX 77204-2020, USA;
vcoulsonthomas@gmail.com,
vjcoulso@central.uh.edu.

MS and SP contributed equally to the work presented here and should therefore be regarded as equivalent authors.

Submitted: October 9, 2018
Accepted: February 12, 2019

Citation: Sun M, Puri S, Mutoji KN, et al. Hyaluronan derived from the limbus is a key regulator of corneal lymphangiogenesis. *Invest Ophthalmol Vis Sci*. 2019;60:1050–1062. https://doi.org/10.1167/iovs.18-25920

Purpose. We recently reported that the glycosaminoglycan hyaluronan (HA), which promotes inflammatory angiogenesis in other vascular beds, is an abundant component of the limbal extracellular matrix. Consequently, we have explored the possibility that HA contributes to lymphangiogenesis in the inflamed cornea.

Methods. To study the role of HA on lymphangiogenesis, we used mice lacking the hyaluronan synthases and injury models that induce lymphangiogenesis.

Results. Here we report that HA regulates corneal lymphangiogenesis, both during post-natal development and in response to adult corneal injury. Furthermore, we show that injury to the cornea by alkali burn upregulates both HA production and lymphangiogenesis and that these processes are ablated in HA synthase 2 deficient mice.

Conclusion. These findings raise the possibility that therapeutic blockade of HA-mediated lymphangiogenesis might prevent the corneal scarring and rejection that frequently results from corneal transplantation.

Keywords: lymphatic vessels, extracellular matrix, glycosaminoglycans, hyaluronan, limbus, inflammation

Lymphatic vessels have vital roles in the drainage of tissue interstitial fluids and the return of inflammatory cell subtypes to the circulation.[1,2] The lymphatics are an integral component of the circulatory system; however, the molecular mechanisms underpinning their development are only now becoming clear. The cornea is an immunologically and angiogenically privileged tissue, and therefore lacking both blood and lymphatic vessels, although lymphatic vessels drain the nearby limbal region and the adjacent subconjunctiva.[3,4] The limbus forms the border between the transparent cornea and the conjunctiva, separating the optically clear cornea from the opaque sclera.[5] The limbus contains blood vessels and lymphatic vessels that arise primarily from the anterior ciliary arteries and lymphatic vessels, which are connected to the conjunctival lymphatic network.[6] Lymphatic and blood vessels are not distributed homogeneously within the limbus but rather predominate within the nasal region, where they proliferate in response to inflammation and injury.[2,6]

The lymphatic system has an important role in regulating inflammation, immunity, and tissue repair after injury. Moreover, inflammatory stimuli may themselves trigger the sprouting of new lymphatic vessels in a process termed *lymphangiogenesis*.[7] The outgrowth of such vessels from the limbus into the central cornea can lead to reduced transparency and consequent reduction of visual acuity. Hence, corneal lymphangiogenesis and angiogenesis lead to the loss of both immune privilege and vision. Substantial evidence suggests that lymphangiogenesis is a strong risk factor for corneal transplantation rejection, and recent studies have shown that inhibiting corneal neovascularization can promote graft survival in a murine model of corneal transplantation.[8,9] Indeed, corneal blindness due to scarring, lymphangiogenesis, and angiogenesis is currently the fourth leading cause of vision loss worldwide. Consequently, an adequate understanding of biological processes that regulate the formation of new lymphatic and blood vessels after injury is imperative for the development of potential new therapies.

The precise regulatory mechanisms that govern lymphangiogenesis are yet to be fully understood. The vascular endothelial growth factor (VEGF) family members—namely VEGF-A, -B, -C, and -D—have been shown to mediate angiogenesis and lymphangiogenesis.[10,11] Seminal studies have shown that VEGF-C has an important role in stimulating lymphatic endothelial cell (LEC) growth.[12,13] Further studies have shown that lymphangiogenesis is primarily mediated by VEGF-C and -D, which bind the tyrosine kinase linked receptor VEGFR3 expressed by LECs.[14,15] Both hypoxia and inflammation trigger the release of members of the VEGF family from inflammatory cells to stimulate angiogenesis and lymphangiogenesis. Studies have shown that other growth factors including hepatocyte growth factor (HGF), insulin-like growth factors 1 and 2, platelet-derived growth factor B (PDGF-B), and fibroblast growth factor (FGF) also regulate proliferation, migration, and survival of LECs either in a VEGFR-3-independent or -dependent manner.[16,17]

For decades, research into the mechanisms of lymphangiogenesis has been limited by the difficulty of visualizing lymphatic vessels in tissues.[18,19] However, in recent years, a number of highly specific lymphatic vessel markers have been identified—most notably, the lymphatic vessel endothelial hyaluronan receptor 1 (LYVE-1),[20] a close relative of the leucocyte HA receptor CD44.[21] Recently, LYVE-1 was shown to mediate the entry and trafficking of dendritic cells via lymphatic vessels, as well as lymph-borne clearance of inflammatory macrophages from the infarcted myocardium through interaction with HA in the leucocyte surface glycocalyx.[22,23] Importantly, the interaction of LYVE-1 with low molecular weight HA (LMWHA) oligosaccharides has also been shown to transduce signals for lymphangiogenesis and lymphatic endothelial cell migration in vitro through the phosphorylation of both ERK1/2 and PKC α/β II in LECs.[24] However, whether HA has a role in lymphatic vessel development or inflammatory lymphangiogesis in vivo remains unknown.

HA is a high molecular weight glycosaminoglycan (GAG) composed entirely of repeating disaccharide units of D-glucuronic acid (GlcA) and N-acetylglucosamine (GlcNAc), which are alternately linked by β-1,3- and β-1,4-glycosidic bonds. HA is naturally synthesized by a class of integral membrane proteins called hyaluronan synthases (HASs), of which vertebrates have three types: HAS1, HAS2, and HAS3. Studies have shown that primarily two forms of HA are produced by HAS enzymes: high molecular weight HA (HMWHA) of approximately 2000 kDa and LMWHA of approximately 200 kDa. The size of the HA chains range from HMWHA to LMWHA and can dictate the physiological function and composition of specific HA matrices. We have recently shown[25] that HA matrices are present around umbilical cord mesenchymal stem cells and can actively suppress inflammatory cells, enabling these stem cells to evade host xenograft rejection. We have also shown that a specific type of HA matrix is synthesized by glial cells after brain and spinal cord injury, forming a principal constituent of the glial scar.[26] Further, we have shown that HA regulates limbal stem cell fate in the cornea.[27]

Our recent work in the cornea has demonstrated that HA is present primarily in the limbal region.[27] Given that both lymphatic vessels and HA are present in this region and that such vessels express HA receptors (particularly LYVE-1 at high densities), we investigated whether HA could play a role in regulating corneal lymphangiogenesis. Here, we can now report that HA indeed regulates corneal lymphangiogenesis, both during development and after injury. In addition, we show that during development, HA is present throughout the cornea and that HA matrices can act as platforms for the growth of lymphatic vessels into the cornea. These studies reveal an important role for HA in regulating corneal lymphangiogenesis in the limbal stem cell niche, raising the possibility that a blockade of HA receptor interactions might be used to prevent both corneal scarring after injury and corneal rejection after transplant surgery.

Materials and Methods

Animal Maintenance

To study the role of HA in lymphangiogenesis, knock-out mice for different hyaluronan synthases were used as previously described.[27] In short, combined *Has1*[28] and *Has3*[29] null mice (*HAS1*$^{-/-}$;*HAS3*$^{-/-}$) were generated by mating. Since single constitutive *Has1* and *Has3* null mice are healthy and viable, we opted to maintain these mice as double constitutive knock-out mice. However, *Has2* null mice are embryonic lethal; therefore, conditional knock-out mice were generated to remove *Has2* from the corneal and limbal epithelium. For this task, transgenic mouse lines *K14-rtTA* (stock number 008099) and *tetO-cre* (*TC*) (stock number 006224) were obtained from The Jackson Laboratory and bred with *Has2* floxed mice (*HAS2*$^{flox/flox}$)[30] to generate compound K14-rtTA, tetO-cre, and *HAS2*$^{flox/flox}$ transgenic mice as previously shown.[25,27,31] Administration of doxycycline chow was used to induce K14-driven persistent and irreversible excision of *Has2* in tetratransgenic mice (*K14-rtTA; TC; HAS2*$^{flox/flox}$) generating *HAS2*$^{\Delta/\Delta CorEpi}$. The ablation of *Has2* in K14^{+} cells was induced from embryonic day zero (E0) when dams were placed on doxycycline chow upon mating ad libitum in lieu of regular chow (Dox Diet #AD3008S; Custom Animal Diets, Easton, PA, USA). When combined *K14-rtTA*, *tetO-cre*, and *HAS2*$^{flox/flox}$ mice were fed doxycycline chow, the floxed *Has2* gene was ablated from corneal epithelial cells and limbal epithelial stem cells, generating *HAS2*$^{\Delta/\Delta CorEpi}$ mice. *K14-rtTA*, *tetO-cre*, and *HAS2*$^{flox/flox}$ single or double transgenic mice were used as controls. These littermate controls were housed together with *HAS2*$^{\Delta/\Delta CorEpi}$ mice and also maintained on Doxy chow, ensuring that our observations were not due to the inhibition of inflammation-induced lymphangiogeneis by doxycycline.[32] As mentioned, HA is synthesized by a HAS, of which there are three isoforms; *Has1*, *Has2*, and *Has3*. Our *HAS1*$^{-/-}$;*HAS3*$^{-/-}$ mice express solely HAS2, while the *HAS2*$^{\Delta/\Delta CorEpi}$ mice lack HAS2 expression in K14 expressing cells (which include corneal epithelial and limbal epithelial cells) but HAS2 expression is present in all other cell compartments. *HAS2*$^{\Delta/\Delta CorEpi}$ mice also express HAS1 and HAS3 in all cell compartments (including corneal epithelial and limbal epithelial cells). C57/BL6 mice were obtained from The Jackson Laboratory and were also used as controls. Mice were bred and housed in a temperature-controlled facility with an automatic 12-hour light-dark cycle at the Animal Facility of the University of Houston. The identification of each transgenic allele was determined by PCR genotyping with tail DNA using specific primer pairs. Experimental procedures for handling the mice were approved by the Institutional Animal Care and Use Committee at the University of Houston. Animal care and use conformed to the ARVO Statement for the Use of Animals in Ophthalmic and Vision Research.

Alkali Burn

The alkali burn method used in this study limits the alkali burn area to the central cornea, thereby limiting damage to the limbal stem cell area, as previously discussed.[25] In preparation for the alkali burn, the mice were provided with carprofen gel packs (MediGel CPF; ClearH_2O, Portland, ME, USA) 24 hours before the procedure and maintained on them for 4 days following the procedure. The mice were anesthetized by intraperitoneal injection of ketamine hydrochloride (80 mg/kg) and xylazine (10 mg/kg). The eyes were then rinsed with sterile PBS and topically anesthetized with a drop of proparacaine. Alkali burns were produced by placing a circular 3MM chromatography paper (Whatman, 1-mm diameter; Sigma-Aldrich Corp., St. Louis, MO, USA) previously soaked in 0.1 M sodium hydroxide onto the central cornea for 1 minute and 15 seconds, after which the filter paper was removed and the eye washed continuously with sterile PBS for 1 minute. The corneas were analyzed at 1, 3, 7, 10, and 14 days after alkali burn to study the formation of new lymphatic vessels after injury and ascertain whether lymphangiogenesis is correlated with HA expression. For tissue collection, the mice were euthanized by CO_2 inhalation and the eyeballs enucleated and immersion fixed in 2% buffered paraformaldehyde for 30

minutes. At least six corneas were analyzed for each experimental point.

Intrastromal Injection

In preparation for the intrastromal injection, mice were provided with carprofen gel packs 24 hours before the procedure. Mice were anesthetized by intraperitoneal injection of ketamine hydrochloride (80 mg/kg) and xylazine (10 mg/kg). The intrastromal injection was carried out as previously described.[25] Briefly, a small slit was made in the anterior stroma in the mid-periphery of the cornea with a 27G beveled needle (Monoject, 27G × 1/2"; BD Precisionglide, Becton Dickinson and Co., Franklin Lakes, NJ, USA).

Thereafter, the needle tip was moved sideways to create a small stromal pocket. A blunt 27G needle attached to a 10 µL syringe (Hamilton) was used to inject 2 µL of 0.2% LMWHA, 0.2% HMWHA or PBS (vehicle control) into the corneal stroma of *HAS2*$^{\Delta/\Delta CorEpi}$ mice. The success of the intrastromal injection was monitored by verifying transient opacity in the central cornea immediately after the injection. The procedure was carried out under a ZEISS stemi 508 microscope in sterile conditions. The lymphatic vessel branches were then counted by two independent investigators in a blinded manner. At least six corneas were analyzed for each experimental point.

Corneas Obtained During Different Developmental Time-Points

Heads were obtained from pups at post-natal day 5 (P5), and eyeballs were obtained from mice at P12 and P26. Under a dissection microscope, the eyeball along with the eyelid was removed from P5 heads; thereafter, the eyelid was carefully peeled away and the eyeball separated and dissected to remove the cornea. Four to six corneas were analyzed for each experimental point.

Whole Mount

Mice were euthanized by CO_2 inhalation and eyeballs immediately excised and fixed in 4% paraformaldehyde for 30 minutes. The eyeballs were then washed three times with PBS, treated for 30 minutes with 0.2% sodium borohydride, thereafter extensively washed in PBS. The cornea button was then removed, and subsequently four small peripheral incisions were made to enable flat mount. Corneas were blocked overnight in 10% FBS in PBS containing 0.01 M saponin. Corneas were then incubated overnight with rabbit anti-LYVE-1 (Abcam, ab14917) or biotinylated hyaluronan-binding protein (Millipore, 385911) prepared in block solution at 4°C under agitation. The corneas were then washed in PBS and subsequently incubated with donkey anti-rabbit conjugated with Alexa Fluor 488 (Invitrogen) or Neutravidin555 (Invitrogen) prepared in block solution overnight at 4°C under agitation. Corneas were finally incubated with DAPI and mounted in ProLong Gold antifade reagent (Invitrogen). Entire corneas were scanned under an LSM 800 confocal microscope using the tiling mode and analyzed using the Zen Image software (Zeiss). Multiple z-stack tiles were captured encompassing the entire cornea using either the 10x or 20x objective and frames processed together (using the stitching mode followed by full orthogonal projection) into a single image.

Real-time PCR

Corneas were isolated from *HAS1*$^{-/-}$;*HAS3*$^{-/-}$, *HAS2*$^{\Delta/\Delta CorEpi}$ and wild-type mice 1 week after alkali burn to analyze the expression profile of genes related to hemoangiogenesis, lymphangiogenesis, and inflammation. At least 5 samples were used per experimental point and analyzed separately. The samples were stored at –80°C until mRNA isolation. Total mRNA was isolated from the corneas using Trizol Reagent (Invitrogen, Carlsbad, CA, USA), and RNA concentration and purity were determined using a spectrophotometer at 260 and 280 nm. First strand cDNA was synthesized from 1.5 µg of total RNA using the high capacity cDNA Reverse Transcription kit (Applied Biosystems, catalog 4368814, lot 00593854) according to the manufacturer's instructions. Quantitative real-time PCR amplification was carried out using 50 ng of the cDNA (1:5) and the Powerup SYBR Green Master Mix kit (Applied Biosystems, Catalog number A25918) using a BIO-RAD CXF Connect Real-time System. Amplification consisted of an activation cycle of 95°C for 10 minutes followed by 40 cycles of 95°C for 15 seconds and 60°C for 1 minute. The primer sequences used were Prox1 forward 5′TCACCAGTAAGACATCACCGC3′ and reverse 5′ CTAGAGAGTCCGCTGGCTTG3′, CD31 forward 5′ CTGTGAAAGAGGGGACGAGC3′ and reverse 5′ AGCCTTCCGTTCTTAGGGTCG3′, and IL1β forward 5′ GTGCAAGTGTCTGAAGCAGC3′ and reverse 5′ CTCATCACTGTCAAAAGGTGGC3′. Gene expression levels were normalized against Actβ forward 5′ TCATCCATGGCGAACTGGTG3′ and reverse 5′ CGCAGCCACTGTCGAGTC3′, and GAPDH forward 5′ AACAGCAACTCCCACTCTTC3′ and reverse 5′ CCTGTTGCTGTAGCCGTATT3′ using the $2^{-\Delta\Delta Ct}$ method. The specificity of the amplified products was analyzed through dissociation curves generated by the equipment yielding single peaks.

Lymphatic Endothelial Cells

Primary hDLECs isolated from the dermis of juvenile foreskin were purchased from Promocell (C-12216; Promocell, Heidelberg, Germany), and primary hLLECs isolated from human lymph node were purchased from ScienCell (Cat. No. 2500; Sciencell Research Laboratories, CA, USA). The cells were cultured in Endothelial Cell Basal Medium MV2 with Supplement Mix (C-39221 Promocell) and maintained at 37°C in a humidified incubator under 5% CO_2 with media change every other day. Cells were used for the experiments between passages 4 to 6.

Tube Formation Assay

Fifty µL Matrigel (Ref 356234; Corning, MA, USA) at 4°C was used to coat each well of a 96-well plate and allowed to polymerize at 37°C for 4 hours. A total of 1×10^4 cells were seeded in the presence or absence of 0.05% HMWHA (Part# HA2M-5; Lifecore Biomedical, Chaska, MN, USA), 0.05% LMWHA (Part# HA500K-1; Lifecore Biomedical), 0.05% ULMWHA (Cat# GLR003; R&D Systems, Minneapolis, MN, USA) or 0.5 mM and 1 mM 4-Methylumbelliferone sodium salt >98% (4-MU) (M1508-10G; Sigma-Aldrich). The cells were maintained at 37°C with 5% CO_2. Each condition was tested in triplicate, and three separate experiments were carried out. Cells were observed and imaged with an EVOS microscope immediately and after 4, 16, and 24 hours. Tube formation and other related structures were quantified using image analysis tools. The morphological features of tube formation were quantified using the angiogenesis analyzer plugin for ImageJ by Gilles Carpentier.[33,34] The parameters extracted included the total number of master segments, segments, nodes and junctions.

Investigative Ophthalmology & Visual Science

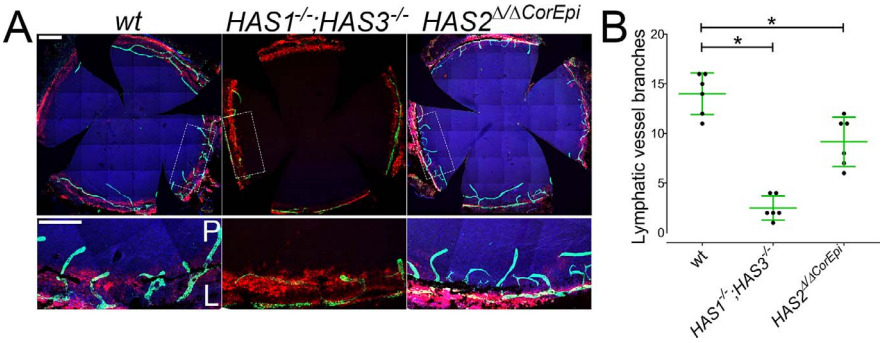

Figure 1. Lymphatic vessel distribution in wild-type, *HAS1*$^{-/-}$;*HAS3*$^{-/-}$ and *HAS2*$^{\Delta/\Delta CorEpi}$ corneas. (**A**) Corneas were obtained and processed for whole mount staining with anti-LYVE-1 (*green*) and HABP (*red*). Zoomed images of the areas demarcated in the *top* panel, which includes the peripheral cornea (P) and limbal region (L), are shown in the *lower* panels. Nuclei were counterstained with DAPI (*blue*). *Scale bar* represents 500 μm. $n = 15$. (**B**) The number of lymphatic vessel branches ≥150 μm was quantified in wild-type, *HAS1*$^{-/-}$;*HAS3*$^{-/-}$ and *HAS2*$^{\Delta/\Delta CorEpi}$ corneas by two independent investigators in a blinded manner.

Effect of HA on Lymphatic Endothelial Cell Proliferation

The effect of HA on the proliferation of hDLECs and hLLECs was determined using the BrdU Cell Proliferation Assay Kit (Cat# 2750; EMD Millipore, MA, USA) according to the manufacturer's protocol. Briefly, hDLECs or hLLECs were seeded in 96-well plates at a density of 5000 cells/well in the presence or absence of 0.05% HMWHA, 0.05% LMWHA, 0.05% ULMWHA, 0.5 mM or 1 mM 4-MU. The cells were incubated at 37°C and 5% CO_2 for 24 hours, after which BrdU was added to the media and the cells incubated for an additional 8 hours. Both media only and cells without the addition of BrdU were used as negative controls. The cells were then fixed and the detection of BrdU incorporation carried out according to the manufacturers' instructions. In short, the cells were incubated with anti-BrdU monoclonal antibody for 1 hour, followed by goat anti-mouse IgG conjugated with peroxidase for 30 minutes at room temperature protected from light. Thereafter, the cells were incubated with TMB peroxidase for 30 minutes at room temperature protected from light followed by the addition of the acid stop solution. Absorbance in each well was read as optical density (OD) using a spectrophotometer microplate reader (FLUOstar Omega; BMG Labtech, Ortenberg, Germany) set at a test wavelength of 450 nm. Each condition was tested in triplicate, and three separate experiments were carried out.

Effect of HA on Lymphatic Endothelial Cell Viability

The cell viability of hDLECs and hLLECs was measured by mitochondrial-dependent reduction of MTT (3-[4,5-dimethylthiazol-2-yl]-2,5-diphenyl-tetrazolium bromide) to purple formazan. The hDLECs or hLLECs were seeded in 96-well plates at a density of 5000 cells/well. The cells were treated or not treated with 0.05% HMWHA, 0.05% LMWHA, 0.05% ULMWHA, 0.5 mM or 1 mM 4-MU and incubated at 37°C and 5% CO_2. After 24 hours, the cells were incubated with MTT solution (M5655; Sigma-Aldrich) (0.5 mg/mL final concentration) for 4 hours at 37°C until a purple precipitate was visible. The solution was carefully removed, and formazan crystals were dissolved in dimethyl sulfoxide (DMSO - 276855-1L; Sigma) for 30 minutes. The formazan product was analyzed by reading absorbance at 570 nm using a spectrophotometer microplate reader (FLUOstar Omega; BMG Labtech).

Results

Influence of HA Synthesis on Normal Corneal Limbal Lymphatic Vessel Growth

To investigate whether HA in the limbal stem cell niche has a role in corneal lymphangiogenesis, we assessed corneal lymphatic vessel distribution in wild-type and *Has*-deficient mice by dual fluorescent immunostaining for LYVE-1 and HA (using anti-LYVE-1 and biotinylated HA binding protein, respectively). Our previous work demonstrated that all three HASs are expressed in the corneal epithelium; therefore, mouse models targeting *Has1-3* were used.[27] These comprised a double *HAS1*$^{-/-}$;*HAS3*$^{-/-}$ constitutive knock-out mouse, and a conditional *HAS2*$^{\Delta/\Delta CorEpi}$ knockout mouse that targeted *Has2* deletion in the corneal epithelium upon doxycycline induction. As shown by images in Figure 1A, both *HAS1*$^{-/-}$;*HAS3*$^{-/-}$ and conditional *HAS2*$^{\Delta/\Delta CorEpi}$ mice present solely vestigial lymphatic vessels within the limbus, indicating that HA synthesis within the limbal region has a role in the development of corneal lymphatic vessels (Figs. 1A, 1B). A rectangular box has been used to demarcate the area shown in higher magnification in the bottom panel (Fig. 1A). The number of lymphatic vessels larger than 150 μm (thereby excluding vestigial vessels) was also quantified in the corneas of wild-type, *HAS1*$^{-/-}$;*HAS3*$^{-/-}$ and *HAS2*$^{\Delta/\Delta CorEpi}$ mice (Fig. 1B). Wild-type mice presented a 3-fold increase in the number of corneal lymphatic vessel branches when compared to *HAS1*$^{-/-}$;*HAS3*$^{-/-}$ and a 1.5-fold increase when compared to *HAS2*$^{\Delta/\Delta CorEpi}$ mice (Fig. 1B). It is important to note that the Schlemm's canal is also located within the limbus, in the irideocorneal angle, and expresses lymphatic marker Prox1, although at lower levels than in lymphatic vessels; however, it does not express LYVE-1.[35–38] Therefore, the Schlemm's canal is not seen in our whole mount images using LYVE-1 staining and was deemed to be beyond the scope of this study.

Influence of HA Synthesis on Alkali Burn-Induced Corneal Lymphangiogenesis

The alkali burn model was used as a means to trigger inflammatory corneal lymphangiogenesis. After alkali burn, wild-type (*wt*) mice displayed a transient increase in HA levels, which extended marginally into the peripheral cornea (seen at 7 days after alkali burn; Fig. 2). This change in HA level was accompanied by a co-ordinate increase in lymphatic vessel sprouting and extension, which could be seen at 7 days, 10

Investigative Ophthalmology & Visual Science

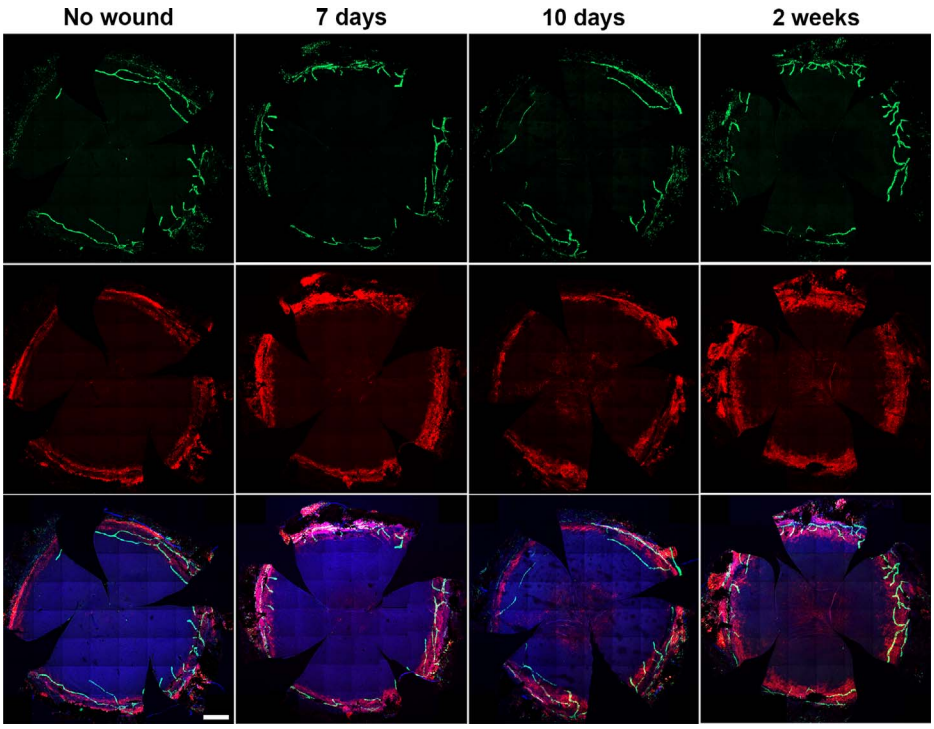

Figure 2. Induction of lymphangiogenesis by alkali burn in wild-type mice. Wild-type mice were subjected to alkali burn and corneas obtained 7 and 10 days and 2 weeks after alkali burn. Uninjured corneas were used as controls. Corneas were obtained and processed for whole mount staining with anti-LYVE-1 (*green*) and HABP (*red*). Nuclei were counterstained with DAPI (*blue*). *Scale bar*: 500 μm. $n = 15$.

days, and 2 weeks after alkali burn (Fig. 2). *HAS1*$^{-/-}$;*HAS3*$^{-/-}$ mice increase HA synthesis throughout the corneal epithelium after alkali burn via *Has2* upregulation (Fig. 3), as previously shown in Gesteira et al.[27] Interestingly, this compensatory increase appeared to exacerbate lymphangiogenesis in the central cornea at 10 days and 2 weeks after alkali burn, as evidenced by the LYVE-1 immunostaining shown in Figure 3. Moreover, these newly extended lymphatic vessels were present exclusively within HA rich areas, suggesting that the glycosaminoglycan may have promoted their proliferation. In contrast, *HAS2*$^{\Delta/\Delta CorEpi}$ mice induced at embryonic day 0 (E0) were unable to upregulate HA synthesis; therefore, they did not exhibit the same lymphangiogenic response after alkali burn (Fig. 4). Curiously, our previous study showed that when

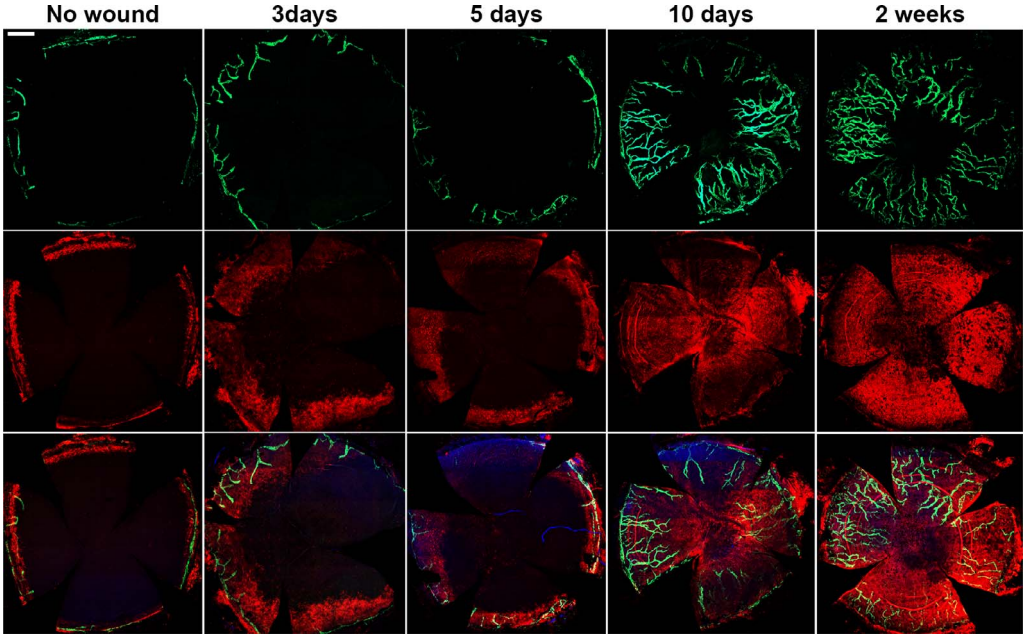

Figure 3. Induction of lymphangiogenesis by alkali burn in *HAS1*$^{-/-}$;*HAS3*$^{-/-}$ mice. *HAS1*$^{-/-}$;*HAS3*$^{-/-}$ mice were subjected to alkali burn and corneas obtained 3, 5, 7, and 10 days and 2 weeks after alkali burn. Uninjured corneas were used as controls. Corneas were obtained and processed for whole mount staining with anti-LYVE-1 (*green*) and HABP (*red*). Nuclei were counterstained with DAPI (*blue*). *Scale bar*: 500 μm. $n = 15$.

Investigative Ophthalmology & Visual Science

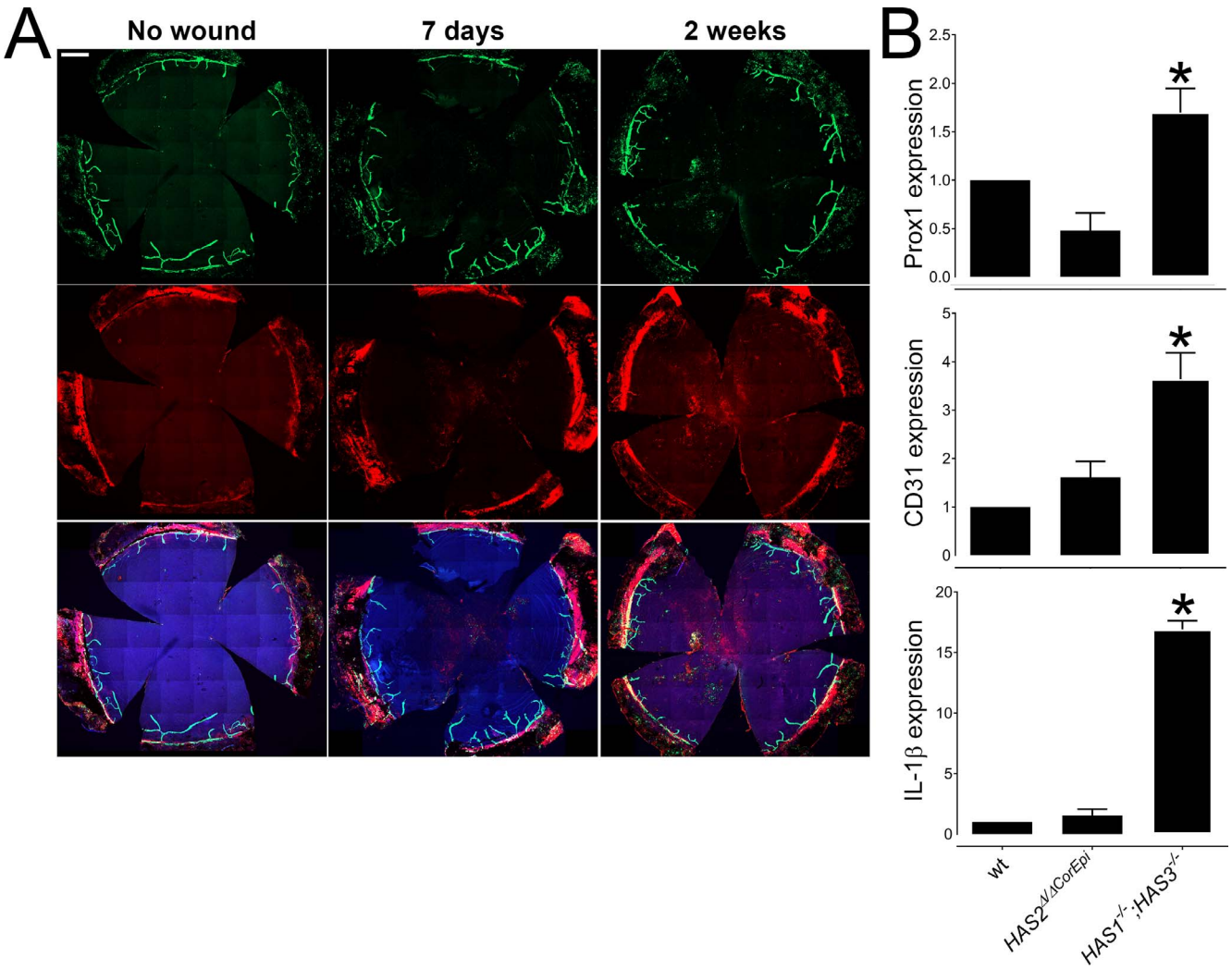

Figure 4. Induction of lymphangiogenesis by alkali burn in *HAS2*$^{\Delta/\Delta CorEpi}$ mice. (**A**) *HAS2*$^{\Delta/\Delta CorEpi}$ mice were subjected to alkali burn and corneas obtained 7 days and 2 weeks after alkali burn. Uninjured corneas were used as controls. Corneas were obtained and processed for whole mount staining with anti-LYVE-1 (*green*) and HABP (*red*). Nuclei were counterstained with DAPI (*blue*). *Scale bar*: 500 µm. $n = 15$. (**B**) the expression profile of Prox1, CD31, and IL-1β were analyzed 1 week after alkali burn in *HAS1*$^{-/-}$;*HAS3*$^{-/-}$, *HAS2*$^{\Delta/\Delta CorEpi}$ and wild-type mice. $n \geq 5$ and *asterisk* represents $P \leq 0.05$.

HAS2$^{\Delta/\Delta CorEpi}$ mice are induced with doxycycline during postnatal stages, they upregulate HA production after alkali burn; however, in the present study, all the *HAS2*$^{\Delta/\Delta CorEpi}$ mice were induced at E0 and displayed only limited HA upregulation after injury.[27]

We further assessed the consequences of alkali burn injury within the corneas of *wt*, *HAS1*$^{-/-}$;*HAS3*$^{-/-}$ and *HAS2*$^{\Delta/\Delta CorEpi}$ mice by quantitive real-time PCR (Fig. 4B). For such, the expression levels of Homeobox Prospero-Like Protein (Prox1), clusters of differentiation 31 (CD31) and Interleukin-1 beta (IL1β) were analyzed to determine the levels of lymphangiogenesis, hemangiogenesis, and inflammation, respectively, 10 days after alkali burn. As seen with immunostaining, *HAS1*$^{-/-}$;*HAS3*$^{-/-}$ mice presented a 1.65-fold increase in Prox1 expression when compared to *wt* mice, while *HAS2*$^{\Delta/\Delta CorEpi}$ mice presented a 0.5 fold decrease in Prox1 expression 10 days after alkali burn. Similarly, *HAS1*$^{-/-}$;*HAS3*$^{-/-}$ mice presented a 3.4 fold increase in CD31 expression when compared to wt mice. However, no statistically significant difference in CD31 expression level was found between *HAS2*$^{\Delta/\Delta CorEpi}$ and *wt* mice. IL1β is a known pro-inflammatory cytokine produced in the cornea after injury, and *HAS1*$^{-/-}$;*HAS3*$^{-/-}$ mice presented a 15-fold increase in IL1β expression when compared to *HAS2*$^{\Delta/\Delta CorEpi}$ and *wt* mice. Thus, our quantitive real-time PCR data corroborated our findings that *HAS1*$^{-/-}$;*HAS3*$^{-/-}$ mice present exacerbated lymphangiogenesis and inflammation after injury.

Induction of Corneal Lymphangiogenesis by Exogenous HA Administration

The majority of *HAS2*$^{\Delta/\Delta CorEpi}$ mice did not present a significant increase in HA synthesis throughout the cornea after alkali burn; consequently, these mice did not display significant corneal lymphangiogenesis after injury. To verify whether the upregulation of HA alone is sufficient to trigger lymphangiogenesis in *HAS2*$^{\Delta/\Delta CorEpi}$ mice, we administered either HMWHA or LMWHA (1% 1.2–1.6 MDa sodium hyaluronate solution and 3% 650–900 kDa sodium hyaluro-

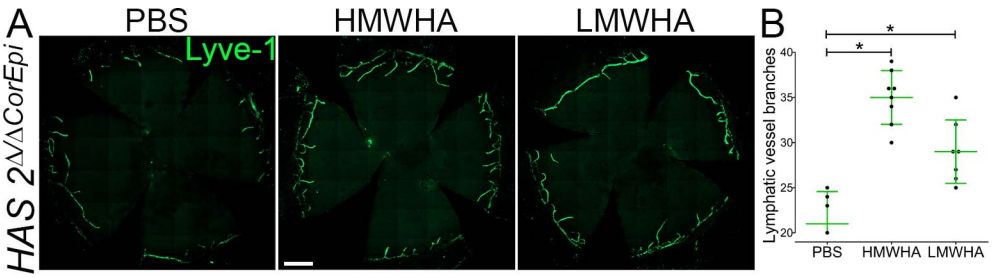

Figure 5. Effect of HA on lymphangiogenesis in $HAS2^{\Delta/\Delta CorEpi}$ mice. (**A**) HA was administered by intrastromal injection into the corneas of $HAS2^{\Delta/\Delta CorEpi}$ mice to verify whether HA alone can trigger lymphangiogenesis. The distribution of lymphatic vessels was analyzed 10 days after administration. Corneas were obtained and processed for whole mount staining with anti-LYVE-1 (*green*). Nuclei were counterstained with DAPI (*blue*). *Scale bar*: 500 μm. (**B**) The number of lymphatic vessel branches after PBS, HMWHA, and LMWHA administration were counted in a double-blinded manner by two independent investigators. $N =$ at least 6 and * represents $P \leq 0.05$. Data represent the mean ± SD of the total number for each condition.

nate solution, respectively [Lifecore Biomedical]) into the corneas of $HAS2^{\Delta/\Delta CorEpi}$ mice via intrastromal injection. We confirmed the molecular weights of the individual HA preparations by high pressure liquid chromatography (HPLC), which yielded a single peak of ~1.4 MDa (peak 1) for HMWHA and a range of sizes from ~750–100 KDa (peak 2–3) with a second peak in the ULMWHA range for LMWHA (peak 4, Supplementary Fig. S1). As shown in Figure 5A, a single intrastromal injection of either HMWHA or LMWHA was sufficient to trigger lymphangiogenesis, whereas injection of PBS alone had no effect. The number of lymphatic vessel branches was quantified (Fig. 5B), revealing an increase in lymphatic vessel extension into the cornea after HMWHA and LMWHA administration. The corneas were analyzed 10 days after the administration of HA and, at this point, there was no longer any detectable HA staining within the cornea, indicating that the administered HA had been absorbed during the 10-day period.

HA Distribution During Post-Natal Corneal Lymphatic Development

Our data show that under conditions of normal homeostasis, $HAS1^{-/-};HAS3^{-/-}$ mice present solely vestigial lymphatic vessels within the corneal limbus when compared to *wt* mice (Fig. 1). To verify the role HA has during normal lymphatic vessel development, we analyzed the distribution of HA and lymphatic vessels in the corneas of *wt*, $HAS1^{-/-};HAS3^{-/-}$ and $HAS2^{\Delta/\Delta CorEpi}$ mice at post-natal days 5, 12, and 26. Interestingly, *wt*, $HAS1^{-/-};HAS3^{-/-}$ and $HAS2^{\Delta/\Delta CorEpi}$ mice all exhibited HA staining throughout the cornea at post-natal day 5 (Fig. 6). Our previously published work and our current findings show that HA is present primarily in the limbal region in adult mouse corneas. Thus, during development of the cornea, HA distribution changes from being present throughout the cornea to being present primarily in the limbal region. In P5 *wt* mice lymphatic vessels developed around the entire circumference of the cornea (Fig. 6). These

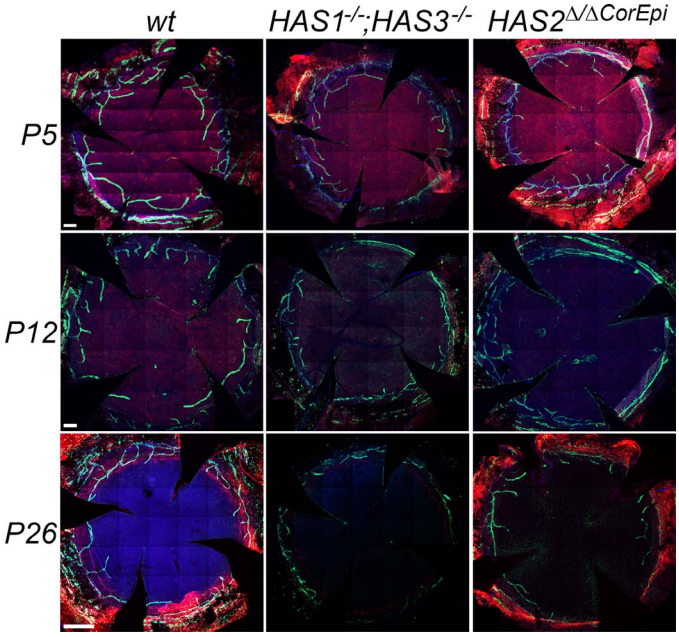

Figure 6. HA and lymphatic vessel distribution in corneas of mice at post-natal days 5, 12, and 26. The distribution of lymphatic vessels was analyzed in wild-type, $HAS1^{-/-};HAS3^{-/-}$ and $HAS2^{\Delta/\Delta CorEpi}$ corneas at post-natal days 5, 12, and 26 (P5, 12 and 26). Corneas were obtained and processed for whole mount staining with anti-LYVE-1 (*green*) and HABP (*red*). Nuclei were counterstained with DAPI (*blue*). *Scale bar* for P5 and P12 represents 200 μm. *Scale bar* for P26 represents 500 μm. $n = 6$.

Investigative Ophthalmology & Visual Science

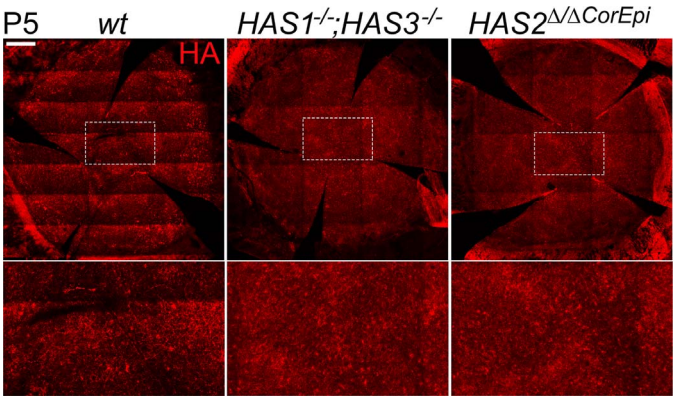

Figure 7. HA distribution in corneas of mice at post-natal day 5. Corneas were obtained and processed for whole mount staining with HABP (*red*). The area demarcated by a *white dashed box* is represented under higher magnification in the *lower* panel. *Scale bar*: 500 µm.

lymphatic vessels are not restricted to the limbal region of *wt* mice at post-natal day 5 and instead extend into the peripheral cornea. Thus, the presence of lymphatic vessels in the early post-natal cornea may have a role in corneal development. *HAS1*$^{-/-}$;*HAS3*$^{-/-}$ and *HAS2*$^{\Delta/\Delta CorEpi}$ mice also have lymphatic vessels extending into the peripheral cornea at post-natal day 5; however, the numbers of lymphatic vessels are significantly reduced when compared to *wt* mice. The distribution of HA throughout the corneas of *wt*, *HAS1*$^{-/-}$;*HAS3*$^{-/-}$ and *HAS2*$^{\Delta/\Delta CorEpi}$ mice at P5 can be seen in more detail in Figure 7 and Supplementary Figure S2. Wild-type mouse corneas present a more organized HA network, when compared to *HAS1*$^{-/-}$;*HAS3*$^{-/-}$ and *HAS2*$^{\Delta/\Delta CorEpi}$ corneas, with visible structures present, including HA rich "net-like" and "cable-like" structures (Fig. 7).

At post-natal day 12, *wt*, *HAS1*$^{-/-}$;*HAS3*$^{-/-}$ and *HAS2*$^{\Delta/\Delta CorEpi}$ mice exhibited a decrease in HA distribution throughout the cornea when compared to post-natal day 5; however, the distribution of HA continues to be throughout the cornea (Fig. 6). Importantly, *wt* mice present higher levels of HA throughout the cornea when compared to *HAS1*$^{-/-}$;*HAS3*$^{-/-}$ and *HAS2*$^{\Delta/\Delta CorEpi}$ mice at P12 (Fig. 6). The overall length of the lymphatic vessel branches that extend into the cornea at P12 is similar to that at P5, indicating there is limited lymphatic vessel growth between post-natal days 5 and 12 (Fig. 6). However, since the corneas increase in size due to the development of the eyeball between P5 and 12, the lymphatic vessels present limited extension into the peripheral cornea at P12 (Fig. 6). It is important to note that mice open their eyes around post-natal day 12.5, which coincides with the decrease in HA expression throughout the cornea and loss of lymphatic vessels extending into the peripheral cornea. *HAS1*$^{-/-}$;*HAS3*$^{-/-}$ and *HAS2*$^{\Delta/\Delta CorEpi}$ mice present a reduced number of lymphatic vessels in the limbal region at post-natal day 12. Therefore, the lymphatic vessels have significantly receded in *HAS1*$^{-/-}$;*HAS3*$^{-/-}$ and *HAS2*$^{\Delta/\Delta CorEpi}$ mice by post-natal day 12, which could be due to the precocious loss of HA. At post-natal day 26 *wt*, *HAS1*$^{-/-}$;*HAS3*$^{-/-}$ and *HAS2*$^{\Delta/\Delta CorEpi}$ corneas display HA expression exclusively in the limbal region and, concomitantly, the lymphatic vessels are restricted to the limbal region. *HAS1*$^{-/-}$;*HAS3*$^{-/-}$ and *HAS2*$^{\Delta/\Delta CorEpi}$ mice present a rudimentary lymphatic vessel network at post-natal day 26 when compared to *wt* mice. It is unclear whether the lymphatic vessels recede between post-natal days 5 and 26, or whether the eye growth which leads to the overall increase in size of the cornea between post-natal days 5 and 26 culminates in the lymphatic vessels becoming restricted to the limbal region.

Influence of HA on In Vitro Lymphatic Vessel Morphogenesis and Proliferation

To further understand the role of HA in the formation of lymphatic vessels, we used the tube formation assay to analyse the process in vitro. Accordingly, human Dermal Lymphatic Endothelial Cells (hDLECs) and human Lymph node Lymphatic Endothelial Cells (hLLECs) were seeded on Matrigel in the presence or absence of HMWHA or the HA biosynthesis inhibitor 4-MU. As shown in Figure 8A and Supplementary Figure S3, administration of HMWHA led to a clear increase in lymphatic vessel growth. This was further confirmed by quantitative analysis using Image J (Supplementary Fig. S4) which revealed significant increases in all aspects of lymphatic vessel formation, including the number of connections between lymphatic vessels (junctions) (Fig. 8B), the number of branches at each connection (nodes) (Fig. 8B), and the number and length of "tube-like structures" (segments) (Figs. 8C, 8D). Thus, HMWHA plays a prominent role in promoting the formation of lymphatic vessels.

In addition to HMWHA, we also compared the effects on lymphangiogenesis of low and intermediate sized HA, namely, HA4, HA8, HA10, HA20, LMWHA, and HMWHA. HMWHA- and LMWHA-treated hDLECs formed an organized lymphatic vessel wall composed of a single continuous endothelial cell layer with a typical 'cobblestone' pattern, evidenced through phalloidin staining (green - Supplementary Fig. S5). In contrast, lymphatic vessel hDLECs cultured in the absence of HA formed "vessel-like" structures in which the endothelial cells were more clustered and had a rounded morphology (Supplementary Fig. S5). Moreover, the efficiency of cobblestone patterned tube formation increased with HA oligosaccharide length (HA20 > HA4, Supplementary Fig. S5).

Interestingly, treatment of hDLECs and hLLECs with the HA synthesis inhibitor 4-MU led to a reduction in viability compared to controls, as assessed by measurement of mitochondrial reductase activity (Figs. 9A, 9B, respectively). A statistically significant difference ($P < 0.05$) was observed between 4-MU treated hDLECs and untreated cells (Fig. 9A). Moreover, the addition of HMWHA partly reversed these effects of 4-MU on viability in the case of both hDLECs and hLLECs (Fig. 9B). Therefore, the loss of HA leads to a decrease in lymphatic vessel endothelial cell viability, which can be rescued by the presence of exogenous HMWHA.

HMWHA and LMWHA treatment increased the proliferation of hDLECs when compared to untreated cells, while 0.5 mM and 1 mM 4-MU treatment had no effect on cell proliferation (Fig. 9C). That said, culturing hLLECs in media containing 0.05% HMWHA increased proliferation when compared to

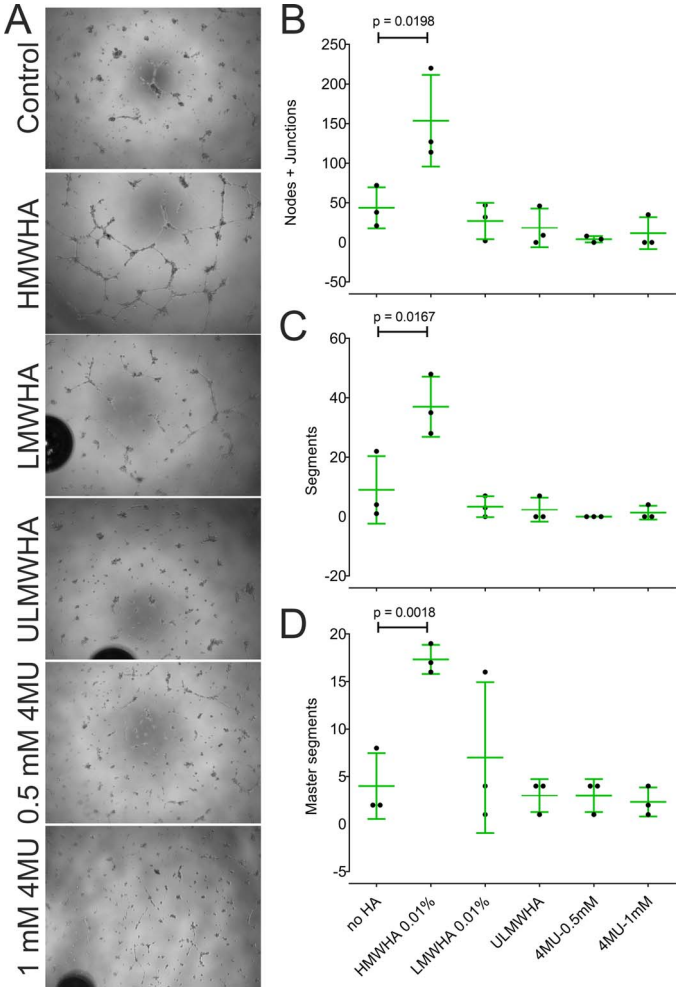

Figure 8. Effect of HA and 4-MU on the formation of "tube-like" structures by hDLECs. (**A**) The tube formation assay was used to study the role of HA on lymphatic vessel formation. The hDLECs were seeded on Matrigel and maintained in the presence or absence of HA or 4-MU. Representative images were acquired of control (untreated), HMWHA, LMWHA, and 1 mM 4-MU-treated hDLECs after 24 hours. (**B–D**) The ability of the hDLECs to assemble into "tube-like" structures was quantified using an imageJ plugin. The quantitative data for number of nodes, junctions, and segments are represented graphically. The experiment was carried out three times in triplicate, and a mean of each experiment is represented in the graph. The mean ± SD of the total number for each condition is represented in *green*.

untreated cells, while 0.05% LMWHA or 0.05% ULMWHA had no effect on cell proliferation (Fig. 9D). Moreover, 4-MU treatment led to a significant drop in hLLEC proliferation, which was reverted by the addition of exogenous HA to the culture media (Fig. 9D). Interestingly, our data show that the effect of HA on lymphatic endothelial cells may vary depending on the origin of the cell line. LMWHA has previously been shown to increase the proliferation of a mouse endothelial cell line isolated from axillary lymph nodes.[24] This study also showed that the effect was dose dependent; LMWHA promoted proliferation at a concentration of 3.13 μg/mL, and this effect was lost at higher and lower concentrations. This study did not, however, examine the effects of HMWHA.

Discussion

This work investigated the role of HA, a major constituent of the limbal stem cell niche, in corneal lymphangiogenesis. Lymphatic vessels are present exclusively in the limbal region of the cornea, and our previously published work demonstrates that HA is also present primarily in this location.[3,27,39] Moreover, limbal lymphatic vessels also express abundant levels of the endothelial HA receptor LYVE-1.[20,40,41] Previous studies have suggested that limbal stem cells and the limbal stem cell niche—located at the intersection between vascularized and non-vascularized tissues—could have a role in regulating lymphangiogenesis and hemangiogenesis,[42] and early reports have suggested that the corneal epithelium acts antiangiogenically.[43,44] Therefore, this study investigated whether HA (which is present in the limbal stem cell niche) could regulate corneal lymphangiogenesis. Interestingly, *HAS1*$^{-/-}$;*HAS3*$^{-/-}$ adult mice, which lack HA in the limbal stem cell niche, assemble only rudimentary lymphatic vessels in the corneal limbus. The inability of these mice to synthesize HA might well explain their failure to form lymphatic vessels. To further understand how HA regulates the growth of lymphatic vessels into the cornea, we used injury models as a means to induce corneal lymphangiogenesis. Our data clearly show that lymphangiogenesis is preceded by an increase in HA levels after injury, and that lymphatic vessels grow exclusively into the HA rich areas. Therefore, after injury, there is an increase in HA production, followed spatio-temporally by the ingrowth of lymphatic vessels.

The lymphatic system has an important role in regulating inflammation, immunity, and tissue repair after injury. The

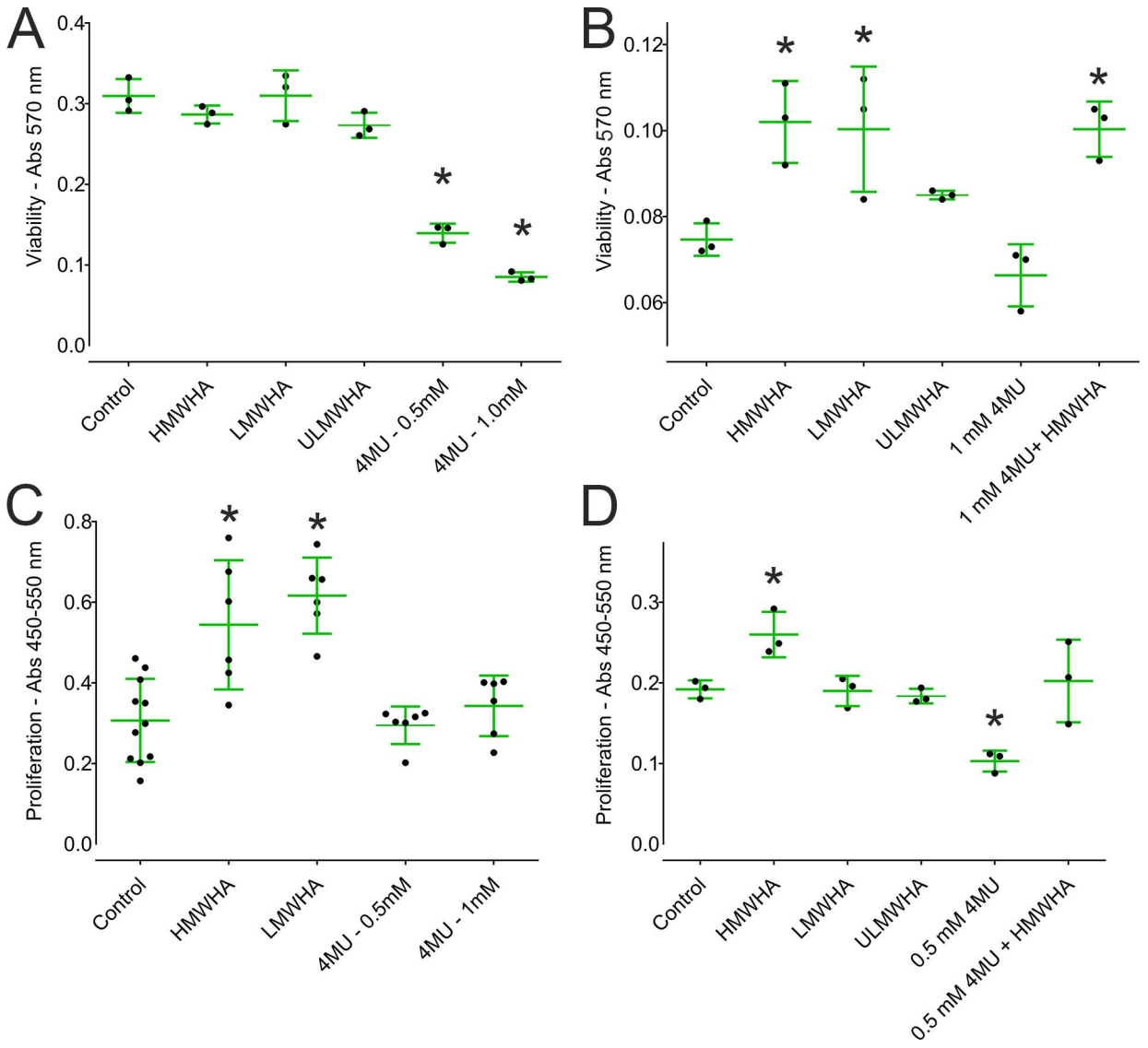

Figure 9. Effect of HA on the viability and proliferation of hDLECs and hLLECs. The MTT assay was used to determine the effect of HA on the viability of hDLECs (**A**) and hLLECs (**B**). Human LECs were incubated for 24 hours in the presence or absence of 0.05% HMWHA, 0.05% LMWHA, 0.05% ULMWHA, 0.5 mM 4-MU or 1 mM 4-MU. Values are expressed as mean ± SD of the optical density (OD) measured at 570 nm. BrdU incorporation was used to determine the effect of HA on the proliferation of hDLECs (**C**) and hLLECs (**D**). LECs were incubated for 24 hours in the presence or absence of 0.05% HMWHA, 0.05% LMWHA, 0.05% ULMWHA, 0.5 mM 4-MU, or 1 mM 4-MU. Thereafter, BrdU was added and the cells incubated for a further 6 hours. BrdU incorporation was detected using the BrdU Cell Proliferation Assay Kit. The mean ± SD of the total number for each condition is represented in *green*. *Asterisks* represents $P \leq 0.05$.

precise regulatory mechanisms that govern lymphangiogenesis after injury remain elusive. Low molecular weight HA fragments (sHA) have been shown to increase VEGF-C–induced LEC proliferation and lymphangiogenesis.[45] HA also acts synergistically with VEGF-C in a renal fibrosis model and increases the expression of VEGF-C in macrophages.[46] Interestingly, *HAS2*$^{\Delta/\Delta CorEpi}$ mice displayed reduced HA synthesis within the cornea; concomitantly, these mice exhibited only limited lymphangiogenesis after alkali burn. These data show that the upregulation of HA synthesis in the cornea is necessary for lymphangiogenesis after injury. Our previously published work shows that all three HAS isoforms are expressed in the cornea, and that after a debridement wound each HAS presents a unique expression pattern.[27] *HAS1*$^{-/-}$;*HAS3*$^{-/-}$ mice present an exacerbated increase in HA synthesis throughout the cornea after alkali burn through *Has2* overexpression, which in turn leads to exacerbated lymphangiogenesis. Given that the loss of *Has2* in the *HAS2*$^{\Delta/\Delta CorEpi}$ mouse model limits HA biosynthesis and, consequently, lymphatic vessel growth, our combined data indicate that HAS2 is the major isoform that regulates corneal lymphangiogenesis. In earlier work, we showed that in the cornea HA is expressed primarily by limbal epithelial cells.[27] Thus, the HA network that supports the growth of lymphatic vessels into the cornea is located in the limbal corneal epithelium. These data have been further confirmed using *HAS2*$^{\Delta/\Delta CorEpi}$ mice. The K14 promoter, which is expressed in the cornea exclusively by epithelial cells, was used as the driver to ablate HAS2 in the cornea. Thus, using this animal model, the *Has2* gene is expressed in all corneal compartments except for the epithelium. Our data show that the corneal epithelium generates the HA network that regulates corneal lymphangiogenesis.

Investigative Ophthalmology & Visual Science

Lymphangiogenesis has been shown to have an important role in a plethora of physiological processes including embryonic and post-natal development.[47] We also investigated the distribution of HA and lymphatic vessels during corneal development. Our study revealed that HA is highly expressed throughout the cornea during early post-natal development. Interestingly, a previous study has reported that there is maximum growth of lymphatic vessels in the central cornea during the period of early post-natal development.[39] Thus, the period of maximum lymphatic vessel growth into the central cornea coincides with the expression of HA throughout the cornea. Importantly, neither *HAS1*$^{-/-}$;*HAS3*$^{-/-}$ nor *HAS2*$^{\Delta/\Delta CorEpi}$ mice exhibited a loss of HA at post-natal day 5, indicating a redundancy/compensatory mechanism among HASs during early developmental stages. However, *HAS1*$^{-/-}$;*HAS3*$^{-/-}$ and *HAS2*$^{\Delta/\Delta CorEpi}$ mice displayed a change in the distribution of HA during early developmental stages, with a loss of HA "net-like" and "cable-like" structures. The change in the organization of the HA network led to a decrease in lymphatic vessel development in both *HAS1*$^{-/-}$;*HAS3*$^{-/-}$ and *HAS2*$^{\Delta/\Delta CorEpi}$ mice. Thus, during corneal development it is possible that the specific spatial-temporal distribution of HASs leads to the formation of an organized HA network that governs the development of lymphatic vessels. The capacity of HA to bind stably to its receptor LYVE-1 in lymphatic vessel endothelium has been shown to depend on the avidity generated by higher-order organization of its glycosaminoglycan ligand either as supramolecular complexes with binding partners such as TSG-6 or as a dense glycocalyx on the surface of migrating leucocytes.[22,48] Only such crosslinked HA configurations have the capacity to cluster LYVE-1 sufficiently for stable adhesion. Nevertheless, even low affinity interactions of LYVE-1 with short HA oligomers can transmit signals for lymphatic endothelial proliferation and motility.[23] We anticipate that the organization of the HA matrix in the developing corneas of *HAS1*$^{-/-}$;*HAS3*$^{-/-}$ and *HAS2*$^{\Delta/\Delta CorEpi}$ mice regulates lymphangiogenesis differently to *wt* mice and speculate that such organization, rather than the presence of HA alone, plays a pivotal role in corneal lymphangiogenesis.

Our developmental studies revealed that during corneal development, HA is expressed throughout the cornea and that the lymphatic vessels grow into a HA-rich cornea. As the cornea develops further, HA expression recedes and is ultimately confined solely to the limbal region, matching the distribution of lymphatic vessels. These findings are in alignment with previous studies, which show that spontaneous lymphatic vessel formation and subsequent regression take place in the cornea during the critical period after birth.[39] Thus, our findings suggest that HA could be an important regulator of lymphatic vessel formation and regression during development. The Cursiefen group has recently shown that corneal lymphatic vessels are also capable of regressing in adult mice after injury.[49] Their study shows that lymphatic vessels regress to levels comparable to uninjured corneas within 4 weeks after a perforating corneal incision injury.[49] Our study shows that lymphatic vessels recede concomitantly with the HA content, becoming located solely in the limbus. Therefore, we can hypothesize that the HA matrix is also necessary for maintaining corneal lymphatic vessels. Targeting the HA matrix could also be explored as a therapy for treating corneas that already present lymphatic vessels in the central cornea.

Until recent identification of lymphatic vessel markers, limited research had been dedicated toward studying lymphatic vessels due to the difficulty of identifying them in tissues. LYVE-1 was identified as a unique marker for lymphatic vessels; thereafter, lymphangiogenesis research grew exponentially.[20,21,50] Although initial studies appeared to indicate that LYVE-1 deficient mice had no obvious defects in normal lymphatic function and development,[51] more recent studies have revealed that the LYVE-1:HA axis has an important role in regulating the entry and trafficking of dendritic cells in the afferent lymphatics under conditions of inflammation.[22,23,52] Whether LYVE-1/HA interactions also play a role in inflammation-induced lymphangiogensis remains elusive. Previous studies have shown that LMWHA promotes LEC proliferation and that such effects are concentration dependent and exerted by small HA (sHA - 4-25 disaccharides in length) but not HMWHA.[24,53] The binding of LMWHA to LYVE-1 is also important for the migration, signal transduction, and tube formation processes involved in lymphangiogenesis.[24] Using lymphangiogenesis assays, lower concentrations of sHA were shown in a recent study to promote the proliferation of lymphatic vessel endothelial cells, while higher concentrations had an inhibitory effect due to the induced expression of TGFβ, a cytokine previously shown to inhibit lymphangiogenesis.[45,54,55] Thus, it was proposed that at higher concentrations, HA-induced TGFβ expression inhibits lymphatic vessel endothelial cell proliferation. These authors also went on to show that the observed stimulatory effect of sHA on LEC proliferation is mediated through LYVE-1, and not CD44 or TLR-4.[45] HA (35-75 kDa) has also been shown to promote lymphangiogenesis and upregulate VEGF-C expression via TLR-4 using a fibrosis model.[46] In our study, the addition of HA (HMWHA, LMWHA, and ULMWHA) to human LECs increased cell proliferation, and the use of 4-MU, a chemical inhibitor that blocks HA synthesis also significantly inhibited cell proliferation. We used the tube formation assay to further investigate the role of HA in lymphangiogenesis. Our data show that human LECs form an organized endothelial cell sheet when exposed to HA, similar to the organization of lymphatic vessels in vivo. However, in the absence of HA, human LECs do not organize into lymphatic vessel-like cell sheets in the same time frame. Therefore, our data show that HA regulates the development and distribution of lymphatic vessels. We postulate that HA could serve as a substrate for lymphatic vessel extension via LYVE-1/HA interaction. We therefore propose that HA serves as a positive regulator of corneal lymphangiogenesis.

Together, our recently published work and current findings demonstrate that HA is expressed throughout the corneal epithelium during development and becomes restricted to the limbus by post-natal day 26. Moreover, HA expression is upregulated in the cornea after injury.[27] Hereby, our findings show that HA distribution throughout the cornea regulates lymphangiogenesis, both during development and after injury. Understanding mechanisms that govern corneal lymphangiogenesis opens new research avenues for the development of specific strategies to limit lymphatic vessel growth, which could be used to prevent corneal scarring after injury and in the management of corneal transplantation rejection. Therefore, limiting HA expression after injury, via *Has2* down-regulation, could provide a means of limiting corneal lymphangiogenesis. This anti-HA treatment could also be extrapolated to limiting tumor growth and metastasis, which rely on angiogenesis and lymphangiogenesis.

Acknowledgments

The authors thank Naoki Itano for kindly providing *Has1* null mice. Supported by start-up funds from the University of Houston, a grant from The Mizutani Foundation to VJCT, a SeFAC awarded to VJCT and the National Institutes of Health/National Eye Institute, Grant R01 EY029289, to VJCT and the Core Grant P30 EY07551. DGJ thanks the UK MRC for support in the form of Unit funding.

The authors acknowledge the use of the Opuntia Cluster and the advanced support from the Center of Advanced Computing and Data Science at the University of Houston.

Disclosure: **M. Sun**, None; **S. Puri**, None; **K.N. Mutoji**, None; **Y.M. Coulson-Thomas**, None; **V.C. Hascall**, None; **D.G. Jackson**, None; **T.F. Gesteira**, None; **V.J. Coulson-Thomas**, None

References

1. Brown P. Lymphatic system: unlocking the drains. *Nature*. 2005;436:456–458.
2. Schulte-Merker S, Sabine A, Petrova TV. Lymphatic vascular morphogenesis in development, physiology, and disease. *J Cell Biol*. 2011;193:607–618.
3. Hos D, Bachmann B, Bock F, Onderka J, Cursiefen C. Age-related changes in murine limbal lymphatic vessels and corneal lymphangiogenesis. *Exp Eye Res*. 2008;87:427–432.
4. Chauhan SK, Dohlman TH, Dana R. Corneal lymphatics: role in ocular inflammation as inducer and responder of adaptive immunity. *J Clin Cell Immunol*. 2014;5:1000256.
5. Van Buskirk EM. The anatomy of the limbus. *Eye (Lond)*. 1989;3(Pt 2):101–108.
6. Iwamoto T, Smelser GK. Electron microscope studies on the mast cells and blood and lymphatic capillaries of the human corneal limbus. *Invest Ophthalmol*. 1965;4:815–834.
7. Maruyama K, Ii M, Cursiefen C, et al. Inflammation-induced lymphangiogenesis in the cornea arises from CD11b-positive macrophages. *J Clin Invest*. 2005;115:2363–2372.
8. Bachmann BO, Bock F, Wiegand SJ, et al. Promotion of graft survival by vascular endothelial growth factor a neutralization after high-risk corneal transplantation. *Arch Ophthalmol*. 2008;126:71–77.
9. Cursiefen C, Cao J, Chen L, et al. Inhibition of hemangiogenesis and lymphangiogenesis after normal-risk corneal transplantation by neutralizing VEGF promotes graft survival. *Invest Ophthalm Vis Sci*. 2004;45:2666–2673.
10. Achen MG, Stacker SA. Tumor lymphangiogenesis and metastatic spread – new players begin to emerge. *Int J Cancer*. 2006;119:1755–1760.
11. Paavonen K, Puolakkainen P, Jussila L, Jahkola T, Alitalo K. Vascular endothelial growth factor receptor-3 in lymphangiogenesis in wound healing. *Am J Pathol*. 2000;156:1499–1504.
12. Breslin JW, Yuan SY, Wu MH. VEGF-C alters barrier function of cultured lymphatic endothelial cells through a VEGFR-3-dependent mechanism. *Lymphat Res Biol* 2007;5:105–113.
13. Dieterich LC, Ducoli L, Shin JW, Detmar M. Distinct transcriptional responses of lymphatic endothelial cells to VEGFR-3 and VEGFR-2 stimulation. *Sci Data*. 2017;4:170106.
14. Makinen T, Veikkola T, Mustjoki S, et al. Isolated lymphatic endothelial cells transduce growth, survival and migratory signals via the VEGF-C/D receptor VEGFR-3. *EMBO J*. 2001;20:4762–4773.
15. Han KY, Chang JH, Dugas-Ford J, Alexander JS, Azar DT. Involvement of lysosomal degradation in VEGF-C-induced down-regulation of VEGFR-3. *FEBS Lett*. 2014;588:4357–4363.
16. Cueni LN, Detmar M. New insights into the molecular control of the lymphatic vascular system and its role in disease. *J Invest Dermatol*. 2006;126:2167–2177.
17. Skobe M, Hamberg LM, Hawighorst T, et al. Concurrent induction of lymphangiogenesis, angiogenesis, and macrophage recruitment by vascular endothelial growth factor-C in melanoma. *Am J Pathol*. 2001;159:893–903.
18. Munn LL, Padera TP. Imaging the lymphatic system. *Microvasc Res*. 2014;96:55–63.
19. Yousefi S, Zhi Z, Wang RK. Label-free optical imaging of lymphatic vessels within tissue beds in vivo. *IEEE J Sel Top Quantum Electron*. 2014;20:6800510.
20. Banerji S, Ni J, Wang SX, et al. LYVE-1, a new homologue of the CD44 glycoprotein, is a lymph-specific receptor for hyaluronan. *J Cell Biol*. 1999;144:789–801.
21. Prevo R, Banerji S, Ferguson DJ, Clasper S, Jackson DG. Mouse LYVE-1 is an endocytic receptor for hyaluronan in lymphatic endothelium. *J Biol Chem*. 2001;276:19420–19430.
22. Johnson LA, Banerji S, Lawrance W, et al. Dendritic cells enter lymph vessels by hyaluronan-mediated docking to the endothelial receptor LYVE-1. *Nat Immunol*. 2017;18:762–770.
23. Jackson DG. Hyaluronan in the lymphatics: the key role of the hyaluronan receptor LYVE-1 in leucocyte trafficking [published online ahead of print February 6, 2018]. *Matrix Biol*. https://doi.org/10.1016/j.matbio.2018.02.001.
24. Wu M, Du Y, Liu Y, et al. Low molecular weight hyaluronan induces lymphangiogenesis through LYVE-1-mediated signaling pathways. *PLoS One*. 2014;9:e92857.
25. Coulson-Thomas VJ, Gesteira TF, Hascall V, Kao W. Umbilical cord mesenchymal stem cells suppress host rejection: the role of the glycocalyx. *J Biol Chem*. 2014;289:23465–23481.
26. Coulson-Thomas VJ, Lauer ME, Soleman S, et al. Tumor necrosis factor-stimulated gene-6 (*TSG-6*) Is constitutively expressed in adult central nervous system (CNS) and associated with astrocyte-mediated glial scar formation following spinal cord injury. *J Biol Chem*. 2016;291:19939–19952.
27. Gesteira TF, Sun M, Coulson-Thomas YM, et al. Hyaluronan rich microenvironment in the limbal stem cell niche regulates limbal stem cell differentiation. *Invest Ophthalmol Vis Sci*. 2017;58:4407–4421.
28. Kobayashi N, Miyoshi S, Mikami T, et al. Hyaluronan deficiency in tumor stroma impairs macrophage trafficking and tumor neovascularization. *Cancer Res*. 2010;70:7073–7083.
29. Bai KJ, Spicer AP, Mascarenhas MM, et al. The role of hyaluronan synthase 3 in ventilator-induced lung injury. *Am J Respir Crit Care Med*. 2005;172:92–98.
30. Matsumoto K, Li Y, Jakuba C, et al. Conditional inactivation of Has2 reveals a crucial role for hyaluronan in skeletal growth, patterning, chondrocyte maturation and joint formation in the developing limb. *Development*. 2009;136:2825–2835.
31. Sun M, Puri S, Parfitt GJ, Mutoji N, Coulson-Thomas VJ. Hyaluronan regulates eyelid and meibomian gland morphogenesis. *Invest Ophthalmol Vis Sci*. 2018;59:3713–3727.
32. Han L, Su W, Huang J, Zhou J, Qiu S, Liang D. Doxycycline inhibits inflammation-induced lymphangiogenesis in mouse cornea by multiple mechanisms. *PLoS One*. 2014;9:e108931.
33. Attia M, Scott A, Duchesnay A, et al. Alterations of overused supraspinatus tendon: a possible role of glycosaminoglycans and HARP/pleiotrophin in early tendon pathology. *J Orthop Res*. 2012;30:61–71.
34. Montesano R, Orci L, Vassalli P. In vitro rapid organization of endothelial cells into capillary-like networks is promoted by collagen matrices. *J Cell Biol*. 1983;97:1648–1652.
35. Kizhatil K, Ryan M, Marchant JK, Henrich S, John SW. Schlemm's canal is a unique vessel with a combination of blood vascular and lymphatic phenotypes that forms by a novel developmental process. *PLoS Biol*. 2014;12:e1001912.
36. Park DY, Lee J, Park I, et al. Lymphatic regulator PROX1 determines Schlemm's canal integrity and identity. *J Clin Invest*. 2014;124:3960–3974.
37. van der Merwe EL, Kidson SH. The three-dimensional organisation of the post-trabecular aqueous outflow pathway and limbal vasculature in the mouse. *Exp Eye Res*. 2014;125:226–235.

38. Truong TN, Li H, Hong YK, Chen L. Novel characterization and live imaging of Schlemm's canal expressing Prox-1. *PLoS One*. 2014;9:e98245.
39. Zhang H, Hu X, Tse J, Tilahun F, Qiu M, Chen L. Spontaneous lymphatic vessel formation and regression in the murine cornea. *Invest Ophthalmol Vis Sci*. 2011;52:334–338.
40. Cursiefen C, Schlotzer-Schrehardt U, Kuchle M, et al. Lymphatic vessels in vascularized human corneas: immunohistochemical investigation using LYVE-1 and podoplanin. *Invest Ophthalmol Vis Sci*. 2002;43:2127–2135.
41. Goyal S, Chauhan SK, El Annan J, Nallasamy N, Zhang Q, Dana R. Evidence of corneal lymphangiogenesis in dry eye disease: a potential link to adaptive immunity? *Arch Ophthalmol*. 2010;128:819–824.
42. Notara M, Lentzsch A, Coroneo M, Cursiefen C. The role of limbal epithelial stem cells in regulating corneal (lymph)angiogenic privilege and the micromilieu of the limbal niche following UV exposure. *Stem Cells Int*. 2018;2018:8620172.
43. Kaminski M, Kaminska G, Majewski S. Inhibition of new blood vessel formation in mice by systemic administration of human rib cartilage extract. *Experientia*. 1978;34:490–491.
44. Sekiyama E, Nakamura T, Kawasaki S, Sogabe H, Kinoshita S. Different expression of angiogenesis-related factors between human cultivated corneal and oral epithelial sheets. *Exp Eye Res*. 2006;83:741–746.
45. Bauer J, Rothley M, Schmaus A, et al. TGFbeta counteracts LYVE-1-mediated induction of lymphangiogenesis by small hyaluronan oligosaccharides. *J Mol Med (Berl)*. 2017.
46. Jung YJ, Lee AS, Nguyen-Thanh T, et al. Hyaluronan-induced VEGF-C promotes fibrosis-induced lymphangiogenesis via Toll-like receptor 4-dependent signal pathway. *Biochem Biophys Res Commun*. 2015;466:339–345.
47. Saharinen P, Tammela T, Karkkainen MJ, Alitalo K. Lymphatic vasculature: development, molecular regulation and role in tumor metastasis and inflammation. *Trends Immunol*. 2004;25:387–395.
48. Lawrance W, Banerji S, Day AJ, Bhattacharjee S, Jackson DG. Binding of hyaluronan to the native lymphatic vessel endothelial receptor LYVE-1 is critically dependent on receptor clustering and hyaluronan organization. *J Biol Chem*. 2016;291:8014–8030.
49. Hos D, Bukowiecki A, Horstmann J, et al. Transient ingrowth of lymphatic vessels into the physiologically avascular cornea regulates corneal edema and transparency. *Sci Rep*. 2017;7:7227.
50. Jackson DG. Immunological functions of hyaluronan and its receptors in the lymphatics. *Immunol Rev*. 2009;230:216–231.
51. Gale NW, Prevo R, Espinosa J, et al. Normal lymphatic development and function in mice deficient for the lymphatic hyaluronan receptor LYVE-1. *Mol Cell Biol*. 2007;27:595–604.
52. Vieira JM, Norman S, Villa Del Campo C, et al. The cardiac lymphatic system stimulates resolution of inflammation following myocardial infarction. *J Clin Invest*. 2018;128:3402–3412.
53. Bauer J, Rothley M, Schmaus A, et al. TGFbeta counteracts LYVE-1-mediated induction of lymphangiogenesis by small hyaluronan oligosaccharides. *J Mol Med (Berl)*. 2018;96:199–209.
54. Clavin NW, Avraham T, Fernandez J, et al. TGF-beta1 is a negative regulator of lymphatic regeneration during wound repair. *Am J Physiol Heart Circ Physiol*. 2008;295:H2113–H2127.
55. Oka M, Iwata C, Suzuki HI, et al. Inhibition of endogenous TGF-beta signaling enhances lymphangiogenesis. *Blood*. 2008;111:4571–4579.

Investigative Ophthalmology & Visual Science